

BOUNDING EVIDENCE AND ESTIMATING LOG-LIKELIHOOD IN VAE

A PREPRINT

Łukasz Struski
lukasz.struski@uj.edu.pl

Marcin Mazur
marcin.mazur@uj.edu.pl

Paweł Batorski
pawel.batorski@student.uj.edu.pl

Przemysław Spurek
przemyslaw.spurek@uj.edu.pl

Jacek Tabor
jacek.tabor@uj.edu.pl

Faculty of Mathematics and Computer Science
Jagiellonian University, Kraków, Poland

ABSTRACT

Many crucial problems in deep learning and statistics are caused by a variational gap, i.e., a difference between evidence and evidence lower bound (ELBO). As a consequence, in the classical VAE model, we obtain only the lower bound on the log-likelihood since ELBO is used as a cost function, and therefore we cannot compare log-likelihood between models. In this paper, we present a general and effective upper bound of the variational gap, which allows us to efficiently estimate the true evidence. We provide an extensive theoretical study of the proposed approach. Moreover, we show that by applying our estimation, we can easily obtain lower and upper bounds for the log-likelihood of VAE models.

1 Introduction

Many important models in deep learning [2, 6, 18], reinforcement learning [10, 32, 33] and statistics [11, 17] suffer from the existence of variational gap¹, i.e., a difference between evidence and its lower bound (which follows from Jensen’s inequality):

$$\text{variational gap} = f(\mathbb{E}X) - \mathbb{E}f(X), \quad (1)$$

where X is a random variable and f is a concave function (typically $f = \log$). A simple visualization of this effect is presented in Figure 1.

In the literature, various theoretical approximations of the true evidence $f(\mathbb{E}X)$ exist [8, 16], but are difficult to efficiently use in a deep neural network architecture. One of the reasons is that we train such models on mini-batches, and therefore the standard assumption is that the cost function factorizes as the sum over the input data set. In other words, deep networks naturally minimize (over the networks parameters) the expected value $\mathbb{E}f(X)$, where f is some given function.

However, there often naturally appear situations where minimization of $f(\mathbb{E}X)$ is necessary. Probably the most important such case is the variational autoencoder (VAE) [18],

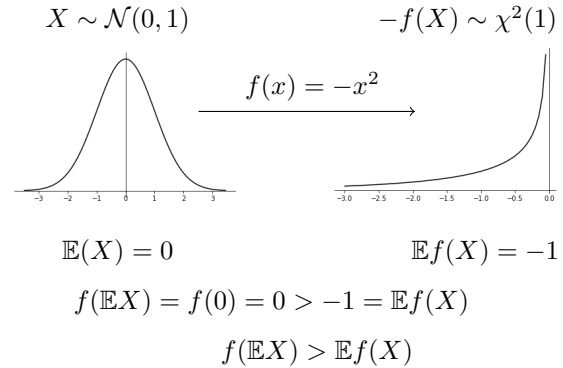


Figure 1: A simple visualization of the variations gap. When we use a concave function $f(x) = -x^2$ to transform Gaussian random variable $X \sim \mathcal{N}(0, 1)$, we can see that $f(\mathbb{E}X) > \mathbb{E}f(X)$.

¹In fact, in such a general context it is rather known as Jensen’s gap, but here and henceforth we call it consequently the variational gap.

which is historically the first and still one of the most popular autoencoder-based generative models. Precisely, VAE uses an encoder network $q(z|x)$, which reduces the dimension of data and produces their latent codes (forcing to follow approximately a given latent prior distribution $p(z)$) and a decoder network $p(x|z)$ that transforms the latent codes back to the data space. Both networks are jointly trained to maximize a variational lower bound for the log-likelihood (the evidence) of data:

$$\text{evidence} = \log \mathbb{E}_{z \sim q(\cdot|x)} \frac{p(x|z)p(z)}{q(z|x)}, \quad (2)$$

which is known as evidence lower bound or (briefly) ELBO:

$$\text{ELBO} = \mathbb{E}_{z \sim q(\cdot|x)} \log \frac{p(x|z)p(z)}{q(z|x)}. \quad (3)$$

The use of ELBO, instead of a direct value of log-likelihood, seems to be a fundamental problem in VAE. In practice, such optimization can lead to learning suboptimal parameters [6], when we mean that our final goal is an approximation of data distribution. Hence, estimating, bounding, and reducing a difference between the true evidence and ELBO, i.e., the variational gap, became important issues investigated so far by many authors from the machine learning community (see the paragraph *Variational gap* in Section 2 for respective overview of the literature). Moreover, such problems are (in a general context) strictly related to those concerning (reversed) Jensen’s inequality, which is a subject of studies in the field of pure and applied mathematics, including statistical inference (see the paragraph *Jensen’s inequality* in Section 2 for appropriate references).

In our work, we provide an extensive theoretical approach regarding the variational gap. In particular, we construct novel upper bounds for $f(\mathbb{E}X)$ (and hence also for the size of variational gap), which are given as expected values of some random variables that depend on X , and then combine them with the technique inspired by [6], to prove tighter bounds for the exact value of $f(\mathbb{E}X)$. Additionally, as an application in the field of deep learning, we use these general results for precise estimating of log-likelihood for generative models, which are designed to learn only some lower bounds. Consequently, we obtain a method that allows comparing the effectiveness of the training process, which we examine using a few different experimental settings, involving VAE-like architectures, i.e. the classical (Gaussian) VAE and two variants of the importance weighted (Gaussian) autoencoder (IWAE) [6], all trained on MNIST, SVHN, and CelebA datasets.

Our contribution can be summarized as follows:

- we introduce novel upper bounds for the variational gap, which allows us to calculate tight rigorous estimation of $f(\mathbb{E}X)$ for any concave function f ,
- we apply these results for $f = \log$, to provide precise estimates for the true evidence (log-likelihood) of data, which we treat as a practical method for validating the effects of training in generative models involving lower bound optimization,
- we perform experiments that examine the use of the obtained technique to compare between three learned Gaussian autoencoders, i.e. classical VAE and two different IWAE models, on MNIST, SVHN and CelebA datasets.

2 Related work

Variational gap One of the most popular generative, autoencoder-based models is variational autoencoder (VAE) [18] which aims to maximize log-likelihood of the data. However, since this likelihood is intractable, the main idea which stays behind estimating it is to calculate and optimize evidence lower bound (ELBO) instead, which results in appearing the variational gap.

One of the problems with variational gap is its behavior, since it can be tiny or tremendous, depending on data distribution. The importance of taking care of gaps and their possible offending effects was mentioned in [2]. There are several techniques to deal with the variational gap, such as its direct estimation [1] or finding an upper or lower bound, to know how much we can lose. There are several approaches to bound variational gap, e.g., [28] and [22] create lower bounds using big-O notation. Bounds for the variational gap were also derived by [17], who later used them for deriving new inequalities (e.g. bounding Csiszár divergence or converse of the Hölder inequality). Other approaches were introduced in [8], where the authors proposed χ upper bound (CUDO) for the evidence of the data that was also used to estimate the marginal log-likelihood, and in [16], where the evidence upper bound (EUBO) is proposed and used for the estimation of Bayesian logistic regression and Bayesian neural networks. Other upper bounds were also proposed in [12] or [23].

Let us also note that we can find a broad usage of variational inference not only in the context of generative models. For example, [33] use it to present the expectation maximization algorithm (EM) for computing optimal policies by solving Markov decision processes. Furthermore, [4] say that people use probabilistic inference when they plan, [20] uses

variational inference to derive a new view of reinforcement learning, where decision making is an inference problem represented in a type of graphical model, and [10] proposes a policy optimization algorithm in the context of variational inference.

Jensen’s inequality Convex functions become interesting objects in deep learning, due to their essential features, such as easiness in finding global minimum or transforming into concave functions. Their importance is often the result of Jensen’s inequality, its reversed version, and refinements. The problems related to Jensen’s inequality have also been subjects of intensive studies in other scientific fields, including pure and applied mathematics [5, 13, 31], statistical inference [9, 15, 27], reinforcement learning [7, 34], or even biological studies [30].

3 Theoretical study

In this section, we present the main theoretical results of the paper. In the first subsection, in Theorem 3.1 and Corollary 3.4 we derive a general condition which, under the assumption of concavity, enables to estimate the evidence from above. In the second subsection, we describe the technique inspired by [6], where it was used in a special case, which allows us to decrease the size of the gap by replacing the random variable with the mean of its independent copies. The third subsection contains the crucial result of the paper Theorem 3.7, in which we provide a large class of upper estimations of the evidence. By respectively, choosing the parameter C in Theorem 3.8, this allows us to obtain for the map $f = \log$ much tighter estimations than those given directly by Corollary 3.4, see Section 4. In the last subsection, we try to answer the question of where the true evidence lies in the interval given by the lower bound and the upper bound. In particular, we show in Theorem 3.11 that for an important class of log-normal distributions, the true evidence lies exactly in the middle of that interval.

3.1 Variational gap

Let X be a random variable. By the classical Jensen inequality, for every concave function f we have $f(\mathbb{E}X) \geq \mathbb{E}f(X)$. Our aim is to obtain (under the above general assumptions) an upper bound for $f(\mathbb{E}X)$, which requires computing only the expected value of some random variable that depends on X . (Note that such an additional supposition ensures the additivity of such a bound when applied for solving optimization problems by machine learning algorithms). This easily follows from the following theorem which can also be found in [9], in a more general form. Nevertheless, for the completeness, we include the proof in the supplementary material.

Theorem 3.1. *Let f be a smooth concave function. Then*

$$f(\mathbb{E}X) \leq \mathbb{E}(f(X) + (Y - X)f'(X)), \quad (4)$$

where X and Y are two independent random variables with the same distribution.

Theorem 3.1 and Jensen’s inequality $f(\mathbb{E}X) \geq \mathbb{E}f(X)$ imply that the true value of $f(\mathbb{E}X)$ is enclosed in the interval

$$[\mathbb{E}f(X), \mathbb{E}f(X) + \mathbb{E}((Y - X)f'(X))]. \quad (5)$$

Thus, the size of the variational gap is bounded from above by the length of the interval (5), i.e. by the value of $\mathbb{E}[(Y - X)f'(X)]$.

Now let us proceed to the most important case of $f = \log$. By applying Jensen’s inequality and Theorem 3.1 we directly obtain the following corollary.

Corollary 3.2. *We have*

$$\mathbb{E} \log X \leq \log \mathbb{E}X \leq \mathbb{E} \log X + \mathbb{E} \frac{Y}{X} - 1, \quad (6)$$

where X and Y are independent random variables with the same distribution.

3.2 Reducing variational gap

In this subsection, we apply the technique inspired by [6], to obtain a tighter (additive) estimation of $f(\mathbb{E}X)$. It comes down to use (instead of X) the random variable

$$\bar{X}_k = \frac{1}{k}(X_1 + \dots + X_k), \quad (7)$$

representing the mean of a k -sample from X (consisting of k independent copies of X). Clearly, $\mathbb{E}\bar{X}_k = \mathbb{E}X$, which implies that $f(\mathbb{E}\bar{X}_k) = f(\mathbb{E}X)$. The following theorem is (in fact) a part of Theorem 1 from [6], restated in a general setting. However, for completeness, we include a novel proof in the supplementary material.

Theorem 3.3. *Let X be a random variable, and let f be a continuous concave function. Then (using the notation given in (7)) for every $k > 0$ we have*

$$\mathbb{E}f(\bar{X}_k) \leq \mathbb{E}f(\bar{X}_{k+1}). \quad (8)$$

Moreover, if the support of X is contained in some closed bounded interval lying in the domain of f , then

$$\lim_{k \rightarrow \infty} \mathbb{E}f(\bar{X}_k) = f(\mathbb{E}X). \quad (9)$$

Assuming bounded support for X in Theorem 3.3 we followed (Burda et al., 2015), where the respective theory behind the use of the k -sample technique is based on this assumption and illustrates the underlying case in a simplified setting. Although the theorem may “survive” in the more general case (as shown below in the example involving the Gamma distribution), the proof would, however, cause some technical difficulties, resulting in reducing the clarity of the presentation.

Applying (5) to the random variable \bar{X}_n , we obtain the following

$$f(\mathbb{E}X) \in [\mathbb{E}f(\bar{X}_k), \mathbb{E}f(\bar{X}_k) + \mathbb{E}((\bar{Y}_k - \bar{X}_k)f'(\bar{X}_k))], \quad (10)$$

where X and Y are independent random variables from the same distribution, and X_1, \dots, X_k and Y_1, \dots, Y_k are independent copies of X and Y , respectively. By Theorem 3.3 the left end of the above interval converges to $f(\mathbb{E}X)$. Hence, a natural question arises, whether the same happens for the right end. In the following corollary, we show that this is the case.

Corollary 3.4. *Let X be a random variable and let f be a concave function such that $(m - x)f'(x)$ is convex for arbitrary m in the support of X . Then the width of the interval given in (10), i.e. $\mathbb{E}((\bar{Y}_k - \bar{X}_k)f'(\bar{X}_k))$, is a decreasing sequence with k . Moreover, if the support of X is contained in the closed bounded interval lying in the domain of f' , then the limit is 0.*

Proof. It is enough to apply Theorem 3.3 for the concave function: $-(\mathbb{E}X - x)f'(x)$. \square

Note that although we outlined a possibility of using Corollary 3.4 to make the size of a variational gap arbitrary small in the case when we cannot bound values of X almost surely in the domain of f' , this technique still has some limitations. Indeed, if, for example, $X \sim \text{Gamma}(a, \theta)$ and $f = \log$, then $\bar{X}_k \sim \text{Gamma}(ka, \theta/k)$ and $1/(\bar{X}_k) \sim \text{Inv-Gamma}(ka, k/\theta)$, where $\text{Gamma}(a, \theta)$ and $\text{Inv-Gamma}(a, \theta)$ denote Gamma and Inverse-Gamma distributions with the shape parameter $a > 0$ and the scale parameter $\theta > 0$, respectively. Therefore, we can calculate:

$$\mathbb{E}((\bar{Y}_k - \bar{X}_k)f'(\bar{X}_k)) = \mathbb{E}(Y)\mathbb{E}(\frac{1}{\bar{X}_k}) - 1 = \frac{a\theta k}{\theta(ka-1)} - 1 = \frac{1}{ka-1}, \quad (11)$$

provided $ka > 1$. Now, even though this means that we can find k large enough to decrease a variational gap sufficiently, we see that when the value of a approaches 0 we may obtain an enormous gap even for a large k . Taking into consideration the properties of the Gamma distribution, this phenomenon means that when we sample from X , we obtain arbitrary small (positive) values more and more likely. In practice, such a situation may appear in a VAE setting when we are dealing with outliers, which is a direct motivation for the improvement introduced in the next subsection.

3.3 Improved bounds for variational gap

In this subsection, we provide another technique, which is crucial in the estimation of the size of the variational gap and addresses the problem described at the end of the previous subsection. Although we start with a general proposition, which idea lies in generalizing the estimations obtained by the concavity, we eventually fix our attention on the case $f = \log$.

Proposition 3.5. *Assume that f , g , and h are arbitrary functions such that*

$$f(a) \leq g(x) + ah(x) \text{ for every } a \text{ and } x. \quad (12)$$

Then

$$f(\mathbb{E}X) \leq \mathbb{E}(g(X) + Yh(X)), \quad (13)$$

where X and Y are two independent random variables with the same distribution.

Proof. The proof follows the same lines as the proof of Theorem 3.1. We consider the probabilistic space (Ω, μ) and independent random variables $X, Y: \Omega \rightarrow \mathbb{R}$ with the same distribution. We use the notation

$$m = \mathbb{E}X = \int_{\Omega} X d\mu. \quad (14)$$

Clearly $\mathbb{E}X = \mathbb{E}Y$. Observe that, by the assumptions, for every $\omega \in \Omega$ we have

$$f(m) \leq g(X(\omega)) + mh(X(\omega)). \quad (15)$$

Integrating the above formula over all $\omega \in \Omega$, we get

$$\begin{aligned} f(\mathbb{E}X) &= \int_{\Omega} f(m) d\mu \leq \int_{\Omega} g(X(\omega)) + mh(X(\omega)) d\mu \\ &= \mathbb{E}g(X) + \mathbb{E}Y\mathbb{E}h(X) = \mathbb{E}(g(X) + Yh(X)), \end{aligned} \quad (16)$$

which ends the proof. \square

Now we focus our attention on the case when $f = \log$. We prove that given an arbitrary function g , we can easily compute the optimal h .

Lemma 3.6. *Let $g: (0, \infty) \rightarrow \mathbb{R}$ be an arbitrary function. Then*

$$\log a \leq g(x) + a \exp(-g(x) - 1) \text{ for all } a, x > 0. \quad (17)$$

Moreover, for any function $h: (0, \infty) \rightarrow \mathbb{R}$ satisfying

$$\log a \leq g(x) + ah(x), \quad (18)$$

we have

$$h(x) \geq \exp(-g(x) - 1). \quad (19)$$

Proof. Consider an arbitrary function h . Let $x > 0$ be fixed. We are going to find an equivalent condition for h so that

$$\log a \leq g(x) + ah(x) \text{ for all } a > 0. \quad (20)$$

Note that verifying (20) is equivalent to checking whether

$$h(x) \geq \frac{\log a - g(x)}{a} \text{ for all } a > 0, \quad (21)$$

or, equivalently,

$$h(x) \geq \sup_{a>0} \frac{\log a - g(x)}{a}. \quad (22)$$

One can easily check that if $w: (0, \infty) \rightarrow \mathbb{R}$ is a function defined as

$$w(a) = \frac{\log a - g(x)}{a}, \quad (23)$$

then $w'(a) = \frac{1 - (\log a - g(x))}{a^2}$. Consequently, w reaches the maximal value at $a_x = \exp(1 + g(x))$. Thus, the equivalent condition for h to satisfy (20) is

$$h(x) \geq w(a_x) = \exp(-1 - g(x)), \quad (24)$$

which proves all assertions. \square

As a direct consequence of Proposition 3.5 and Lemma 3.6 we obtain the following theorem.

Theorem 3.7. *Let g be an arbitrary function. Then*

$$\log \mathbb{E}X \leq \mathbb{E}(g(X) + Y \exp(-g(X) - 1)), \quad (25)$$

where X and Y are two positive independent random variables with the same distribution.

Now consider a one-parameter family of functions

$$g_C(x) = \log x - 1 + C \quad (C \in \mathbb{R}). \quad (26)$$

Then by applying any function g_C as g in Proposition 3.5, we obtain the following theorem.

Theorem 3.8. *Let C be arbitrarily chosen. Then*

$$\log \mathbb{E}X \leq \mathbb{E} \log X - 1 + C + \exp(-C) \mathbb{E} \frac{Y}{X}, \quad (27)$$

where X and Y are two independent positive random variables with the same distribution.

Observe that by increasing C we can decrease the last component of the right hand side formula in (27). Hence, the optimal value of C (i.e. minimizing the upper bound for $\log \mathbb{E}X$) can be obtained as the one that minimizes the function $W(C) = C + \exp(-C) \mathbb{E} \frac{Y}{X}$. This easily leads to the following corollary.

Corollary 3.9. *Under the assumptions of Theorem 3.8, the optimal value of C is $C = \log \mathbb{E} \frac{Y}{X}$, which gives the following estimates*

$$\mathbb{E} \log X \leq \log \mathbb{E}X \leq \mathbb{E} \log X + \log \mathbb{E} \frac{Y}{X}. \quad (28)$$

Note that Corollary 3.9 cannot be directly applied in our case, as the upper bound for $\log \mathbb{E}X$ provided by (28) does not have an additive form. However, it tells us about the most optimal estimation we can obtain, and hence given the rough initial estimate of $\log \mathbb{E} \frac{Y}{X}$, we can use it as a default value of C in all computations.

3.4 Quality of estimations

We have already proved (see (5)) that for any concave function f we have

$$f(\mathbb{E}X) \in [\mathbb{E}f(X), \mathbb{E}(f(X) + (Y - X)f'(X))], \quad (29)$$

where X and Y are independent random variables with the same distribution. In this section, we are going to show that the optimal choice for an approximation of $f(\mathbb{E}X)$ is the middle of the above interval.

Let us start with the following general result, which relates to a special case of the delta method (see Section 5.3.1 in [3]). For completeness, we include the proof in the supplementary material.

Theorem 3.10. *Assume that f is a smooth function and X and Y are independent random variables with the same distribution, which attain only values ε -close to $\mathbb{E}X$, where $\varepsilon > 0$ is small. Then*

$$f(\mathbb{E}X) = \mathbb{E}f(X) + \frac{1}{2}\mathbb{E}((Y - X)f'(X)) + o(\varepsilon^2). \quad (30)$$

Now we proceed to the case when $f = \log$ and we are going to apply the bounds for \bar{X}_n . Clearly, by the central limit theorem, for large n the distribution of X_n can be considered Gaussian. However, this approximation is not satisfactory from our point of view, since we are limited to the class of positive random variables (which need to be arguments for the log function). Based on the results of [25] (see also [24]), it is known that typically the distribution of the mean of independent positive random variables can be better approximated by the log-normal distribution \mathcal{LN} . In other words, we can write $\bar{X}_n \approx \mathcal{LN}(m, \sigma)$. In the following theorem, we prove that for a log-normal random variable X , the value of $\log \mathbb{E}X$ lies exactly in the middle of the interval given by Corollary 3.9.

Theorem 3.11. *Let X and Y be independent random variables with the same log-normal distribution. Then*

$$\log \mathbb{E}X = \mathbb{E} \log X + \frac{1}{2} \log \mathbb{E} \frac{Y}{X}. \quad (31)$$

Proof. Let $X \sim \mathcal{LN}(m, \sigma)$, which means that $\log X \sim \mathcal{N}(m, \sigma^2)$. Then $\mathbb{E}X = \exp(m + \sigma^2/2)$ and, consequently,

$$\log \mathbb{E}X = m + \frac{\sigma^2}{2}, \quad \mathbb{E} \log X = m. \quad (32)$$

Moreover, $1/X \sim \mathcal{LN}(-m, \sigma)$ and hence

$$\log \mathbb{E} \frac{Y}{X} = \log \mathbb{E}Y + \log \mathbb{E} \frac{1}{X} = m + \frac{\sigma^2}{2} - m + \frac{\sigma^2}{2} = \sigma^2. \quad (33)$$

By applying (32) and (33) in (31), we obtain the conclusion. \square

4 Experiments

In this section, we consider variational generative models (like VAE), let us first establish some standard notation. By $p(x)$ we denote the distribution we construct on the input space $\mathcal{X} = \mathbb{R}^N$. By $p(z)$ we denote the prior distribution on the latent space \mathcal{Z} , while $q(z|x)$ denotes the variational encoder and $p(x|z)$ denotes the variational decoder.

Now, given a point $x \in \mathbb{R}^N$, its model log-likelihood (evidence) is given by

$$\log p(x) = \log \mathbb{E}_{z \sim q(\cdot|x)} \frac{p(x|z)p(z)}{q(z|x)}. \quad (34)$$

To simplify the notation, we put

$$R(x, z) = \frac{p(x|z)p(z)}{q(z|x)}. \quad (35)$$

In the classical VAE model, we maximize

$$\text{ELBO} = \mathbb{E}_{z \sim q(\cdot|x)} \log R(x, z), \quad (36)$$

which is the lower bound for the log-likelihood.

The idea behind the IWAE model [6] is to obtain an (asymptotically optimal) approximation of true evidence by maximizing

$$\text{IW-ELBO}_k = \mathbb{E}_{z_1, \dots, z_k \sim q(\cdot|x)} \log \frac{1}{k} \sum_{i=1}^k R(x, z_i), \quad (37)$$

which is a closer (than ELBO) lower bound for the log-likelihood.



Figure 3: Sampled images for the VAE, IWAE(5) and IWAE(10) models (from left to right) trained on MNIST, SVHN and CelebA datasets (from top to bottom).

To obtain the upper bound for the evidence, which can be additively updated, we use Theorem 3.8 for $X = \frac{1}{k} \sum_{i=1}^k R(x, z_i)$ (where z_i are independently sampled from $q(\cdot|x)$). Then for an arbitrary function $x \rightarrow C_x$ we obtain the estimate

$$GAP_x \leq C_x - 1 + \exp(-C_x) \mathbb{E}_{z_1, \dots, z_k} \left(\frac{\frac{1}{k} \sum_{i=1}^k R(x, \tilde{z}_i)}{\frac{1}{k} \sum_{i=1}^k R(x, z_i)} \right), \quad (38)$$

where the theoretically optimal (i.e. that for which GAP_x is minimal) value of C_x is given by Corollary 3.9.

Thus, our estimating of the log-likelihood is divided into two steps. In the first step, we train a neural network (on the training set) which finds an optimal function C_x . This function C_x gives us important information about the model, as it corresponds to the uncertainty of the prediction. In the second step, we compute the estimations. For the algorithmic details, we refer the reader to the supplementary material.

Case study on synthetic data Suppose that we are given a distribution of data X with known density f . Then obviously, the log-likelihood of data is given by $LL = \int f(x) \log f(x) dx$. Suppose, that using the VAE model we construct the estimation of the data distribution in the class of densities f_θ , where θ denote the weights of the neural networks. Then the evidence of the data X with respect to the density f_θ is, in fact, cross-entropy of the two distributions and is given by the sum of LL and Kullback-Leibler divergence, i.e.

$$\text{evidence} = \int f(x) \log f_\theta(x) dx = LL - D_{KL}(f \| f_\theta). \quad (39)$$

Obviously, if (which is a common case) f does not belong to the family of densities $(f_\theta)_{\theta \in \Theta}$, more precisely $D_{KL}(f \| f_\theta) > 0$, then evidence $< LL$. Since we used the VAE model, we also have ELBO (estimated from the cost function), which clearly satisfies $ELBO < \text{evidence}$. Finally, by applying our above estimations we can obtain upper and lower bounds for the evidence of data, which become tighter with the increasing of number of samples k , chosen for each x from the distribution $q(\cdot|x)$.

We illustrate the above reasoning in the case of simple synthetic one-dimensional data generated from the Laplace distribution $X \sim \text{Laplace}(0, 0.2)$. We used the VAE model (for architecture details, see the supplementary material)

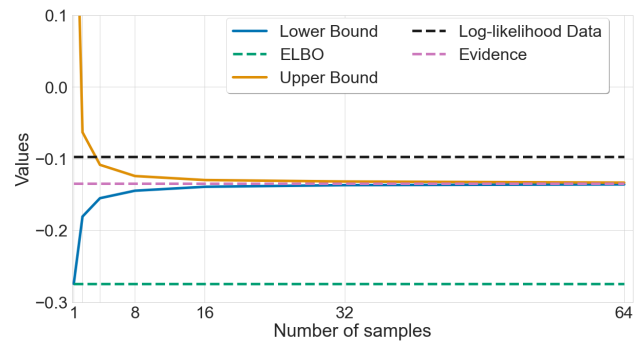


Figure 2: Behavior of the lower and the upper bounds for the evidence vs. number of draws from the latent.



Figure 4: Images sorted (increasingly) by the value of parameter C for VAE (the first two rows), IWAE(5) (the second two rows), IWAE(10) (the last two rows) trained on SVHN and MNIST datasets. Note that these also show the dependence on the size of the variational gap (larger values of C correspond to larger gaps).

with one-dimensional latent space. The experiments are consistent with the above mentioned theoretical discussion, see Figure 2. The true likelihood of the data, coming from the Laplace distribution, equals -0.097 . The ELBO obtained as a value of the cost function of VAE gives a strong lower bound for the log-likelihood of the data. Evidence of the data with respect to the density constructed by VAE lies between ELBO and log-likelihood. Moreover, by applying our approach, we obtain a tight estimate of the evidence, i.e. $\text{evidence} \in [-0.137, -0.132]$, which is calculated for $k = 64$.

Experiments for VAE and IWAE models In our further experiments, we use the improved bounds for the variational gap given in Theorem 3.8. This is caused by the fact that the factor $\mathbb{E}_{\mathcal{X}}^Y$ in (6) is often large (due to the presence of outlier data). Therefore, taking a large C in (27), as was described at the beginning of this section, we can reduce its magnitude. To visualize the impact of C , in Figure 4, we present images from the test set sorted increasingly according to the value of C .

We empirically evaluate the usefulness of the proposed bounds for estimating the model log-likelihood in classical VAE, IWAE(5) ($k = 5$) and IWAE(10) ($k = 10$), each trained on three classical datasets: MNIST [19], SVHN [26], and CelebA [21]. In our calculations, we generate 1024 samples from the latent space of the trained model for each point x_i of data. We repeat the calculation 100 (MNIST), 75 (SVHN) or 25 (CelebA) times, using different random seeds. The code for all experiments is available on the GitHub repository <https://github.com/anonymised>.

We compare the VAE model with IWAE models trained with two different number of samples: $k = 5$ (IWAE(5)) and $k = 10$ (IWAE(10)). For the IWAE models, we took the same neural architectures as we used in VAE.

Table 1: Means and standard deviations of lower and upper bounds for log-likelihood in trained VAE, IWAE(5) and IWAE(10) models, averaged over 10 times evaluations on random seed and 10,000 images from the test sets.

Data	Model	Lower	Upper	Gap
MNIST	VAE	-282.27 ± 0.12	-280.88 ± 0.78	1.57 ± 0.79
	IWAE(5)	-283.97 ± 0.08	-283.82 ± 0.08	0.35 ± 0.03
	IWAE(10)	-283.88 ± 0.11	-283.63 ± 0.09	0.46 ± 0.05
SVHN	VAE	-4015.35 ± 1.02	-4009.94 ± 1.33	5.41 ± 0.53
	IWAE(5)	-3991.28 ± 0.57	-3982.01 ± 3.52	9.27 ± 4.07
	IWAE(10)	-3990.94 ± 0.96	-3981.58 ± 2.72	9.36 ± 1.92
CelebA	VAE	-16141.69 ± 5.193	-16115.50 ± 5.136	26.19 ± 1.683
	IWAE(5)	-16140.56 ± 8.264	-16198.35 ± 8.581	57.79 ± 9.492
	IWAE(10)	-16144.63 ± 7.394	-16206.11 ± 9.424	61.48 ± 8.745

Results Since in VAE like models, we use ELBO as a cost function, we cannot compare models on the true log-likelihood. However, thanks to our approximation, we can calculate the true evidence of data. As a consequence, we can reach such models directly on log-likelihood. Table 1 presents means and standard deviations of estimated lower and upper bounds of the log-likelihood in VAE, IWAE(5) and IWAE(10), all trained on MNIST, SVHN and CelebA.

Note that even though the IWAE model is learned using more latent samples, it not always delivers better results, i.e. greater values of estimates of the log-likelihood (see also [29]). For example, VAE trained on the MNIST dataset obtains the best (the greatest) log-likelihood estimates. We can also observe this effect on randomly generated samples (see Figure 3). Note that this is not the case for the CelebA dataset, where all the results are comparable.

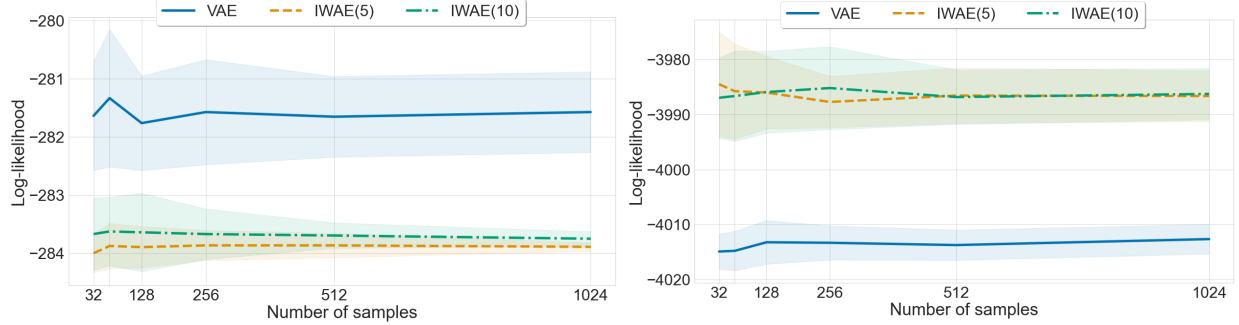


Figure 5: Comparison of lower and upper bounds for log-likelihood obtained in VAE, IWAE(5) and IWAE(10) models, trained on MNIST (on the left) and SVHN (on the right) datasets. Horizontal lines (solid, dashed or dash-dotted) describe centers of intervals between lower and upper bounds, whereas shaded areas show the appropriate ranges.

In Figure 5 we present the dynamics of changes in the lower and upper bound estimates of the log-likelihood for all trained models, depending on the number of sampled points from the latent space (1–1024). It can be easily seen that as the number of samples increases, the size of the gap between the bounds decreases. More detailed results are presented in the supplementary material.

5 Conclusion

In this paper, we proposed novel upper bounds for the variational gap, which allows us to calculate a tight rigorous estimation of $f(\mathbb{E}X)$ for any concave function f with the use of $\mathbb{E}Z$, where Z is a random variable constructed from fixed number of independent copies of X . We focused a particular attention on the most important case, when $f = \log$, where we proposed a new technique which could be adapted to minimize the gap for a given data distribution.

As an application of our method, we showed that we can effectively estimate the lower and the upper bounds for the log-likelihood of various VAE like models, which allows us to compare the evidence of data between different trained models.

References

- [1] Shoshana Abramovich and Lars-Erik Persson. Some new estimates of the ‘jensen gap’. *Journal of Inequalities and Applications*, 2016(1):1–9, 2016.
- [2] Justin Bayer, Maximilian Soelch, Atanas Mirchev, Baris Kayalibay, and Patrick van der Smagt. Mind the gap when conditioning amortised inference in sequential latent-variable models. *arXiv preprint arXiv:2101.07046*, 2021.
- [3] Peter J Bickel and Kjell A Doksum. *Mathematical statistics: basic ideas and selected topics, volumes I-II package*. Chapman and Hall/CRC, 2015.
- [4] Matthew Botvinick and Marc Toussaint. Planning as inference. *Trends in cognitive sciences*, 16(10):485–488, 2012.
- [5] Ilko Brnetić, Khuram Ali Khan, and Josip Pecarić. Refinement of jensen’s inequality with applications to cyclic mixed symmetric means and cauchy means. *J. Math. Inequal*, 9(4):1309–1321, 2015.
- [6] Yuri Burda, Roger Grosse, and Ruslan Salakhutdinov. Importance weighted autoencoders. *arXiv preprint arXiv:1509.00519*, 2015.
- [7] Peter Dayan and Geoffrey E Hinton. Using expectation-maximization for reinforcement learning. *Neural Computation*, 9(2):271–278, 1997.
- [8] Adjani Dieng, Dustin Tran, Rajesh Ranganath, John Paisley, and David M Blei. Variational inference via χ -upper bound minimization. *arXiv preprint arXiv:1611.00328*, 2016.
- [9] Sever Silvestru Dragomir. Some reverses of the jensen inequality with applications. *Bulletin of the Australian Mathematical Society*, 87(2):177–194, 2013.
- [10] XU Duo. Improving actor-critic reinforcement learning via hamiltonian monte carlo method. In *Deep RL Workshop NeurIPS 2021*, 2021.

- [11] Xiang Gao, Meera Sitharam, and Adrian E Roitberg. Bounds on the jensen gap, and implications for mean-concentrated distributions. *arXiv preprint arXiv:1712.05267*, 2017.
- [12] Roger B Grosse, Zoubin Ghahramani, and Ryan P Adams. Sandwiching the marginal likelihood using bidirectional monte carlo. *arXiv preprint arXiv:1511.02543*, 2015.
- [13] László Horváth. Extensions of recent combinatorial refinements of discrete and integral jensen inequalities. *Aequationes mathematicae*, pages 1–21, 2021.
- [14] Sergey Ioffe and Christian Szegedy. Batch normalization: Accelerating deep network training by reducing internal covariate shift. In *International conference on machine learning*, pages 448–456. PMLR, 2015.
- [15] Tony Jebara and Alex Pentland. On reversing jensen’s inequality. *Advances in Neural Information Processing Systems*, pages 231–237, 2001.
- [16] Chunlin Ji and Haige Shen. Stochastic variational inference via upper bound. *arXiv preprint arXiv:1912.00650*, 2019.
- [17] Muhammad Adil Khan, Shahid Khan, and Yuming Chu. A new bound for the jensen gap with applications in information theory. *IEEE Access*, 8:98001–98008, 2020.
- [18] Diederik P Kingma and Max Welling. Auto-encoding variational bayes. *arXiv preprint arXiv:1312.6114*, 2013.
- [19] Yann LeCun, Léon Bottou, Yoshua Bengio, and Patrick Haffner. Gradient-based learning applied to document recognition. *Proceedings of the IEEE*, 86(11):2278–2324, 1998.
- [20] Sergey Levine. Reinforcement learning and control as probabilistic inference: Tutorial and review. *arXiv preprint arXiv:1805.00909*, 2018.
- [21] Ziwei Liu, Ping Luo, Xiaogang Wang, and Xiaoou Tang. Deep learning face attributes in the wild. In *Proceedings of the IEEE international conference on computer vision*, pages 3730–3738, 2015.
- [22] Chris J Maddison, Dieterich Lawson, George Tucker, Nicolas Heess, Mohammad Norouzi, Andriy Mnih, Arnaud Doucet, and Yee Whye Teh. Filtering variational objectives. *arXiv preprint arXiv:1705.09279*, 2017.
- [23] Pierre-Alexandre Mattei and Jes Frellsen. Leveraging the exact likelihood of deep latent variable models. *Advances in Neural Information Processing Systems*, 31, 2018.
- [24] Lilit Mazmanyan, Victor Ohanyan, and Dan Trietsch. The lognormal central limit theorem for positive random variables. Technical report, Working paper. Reproduced within the Research Notes for Appendix A in <http://mba.tuck.dartmouth.edu/pss/>, see also <http://faculty.tuck.dartmouth.edu/images/uploads/faculty/principles-scheduling-scheduling/LognormalCLT.pdf>, 2008.
- [25] Hideaki Mouri. Log-normal distribution from a process that is not multiplicative but is additive. *Physical Review E*, 88(4):042124, 2013.
- [26] Yuval Netzer, Tao Wang, Adam Coates, Alessandro Bissacco, Bo Wu, and Andrew Y Ng. Reading digits in natural images with unsupervised feature learning. 2011.
- [27] Frank Nielsen. A family of statistical symmetric divergences based on jensen’s inequality. *arXiv preprint arXiv:1009.4004*, 2010.
- [28] Sebastian Nowozin. Debiasing evidence approximations: On importance-weighted autoencoders and jackknife variational inference. In *International Conference on Learning Representations*, 2018.
- [29] Tom Rainforth, Adam Kosiorek, Tuan Anh Le, Chris Maddison, Maximilian Igl, Frank Wood, and Yee Whye Teh. Tighter variational bounds are not necessarily better. In *International Conference on Machine Learning*, pages 4277–4285. PMLR, 2018.
- [30] Jonathan J Ruel and Matthew P Ayres. Jensen’s inequality predicts effects of environmental variation. *Trends in Ecology & Evolution*, 14(9):361–366, 1999.
- [31] Tareq Saeed, Muhammad Adil Khan, and Hidayat Ullah. Refinements of jensen’s inequality and applications. *AIMS Mathematics*, 7(4):5328–5346, 2022.
- [32] Emanuel Todorov. General duality between optimal control and estimation. In *2008 47th IEEE Conference on Decision and Control*, pages 4286–4292. IEEE, 2008.
- [33] Marc Toussaint and Amos Storkey. Probabilistic inference for solving discrete and continuous state markov decision processes. In *Proceedings of the 23rd international conference on Machine learning*, pages 945–952, 2006.
- [34] Grady Williams, Nolan Wagener, Brian Goldfain, Paul Drews, James M Rehg, Byron Boots, and Evangelos A Theodorou. Information theoretic mpc for model-based reinforcement learning. In *2017 IEEE International Conference on Robotics and Automation (ICRA)*, pages 1714–1721. IEEE, 2017.

APPENDIX

A Proofs

In this section, we provide proofs omitted from the main article.

Proof of Theorem 3.1. Let (Ω, μ) be a probabilistic space and $X, Y: \Omega \rightarrow \mathbb{R}$ be independent random variables with the same distribution. We use notation

$$m = \mathbb{E}X = \int_{\Omega} X d\mu. \quad (40)$$

Clearly $\mathbb{E}X = \mathbb{E}Y$. Observe that applying Taylor's expansion and concavity of f (which means that $f'' \geq 0$), for every $\omega \in \Omega$ we have

$$f(m) \leq f(X(\omega)) + (m - X(\omega))f'(X(\omega)). \quad (41)$$

Integrating the above formula over all $\omega \in \Omega$ and making use the fact that X and Y are independent random variables with the same distribution, we obtain

$$\begin{aligned} f(\mathbb{E}X) &= \int_{\Omega} f(m) d\mu \leq \int_{\Omega} f(X(\omega)) + (m - X(\omega))f'(X(\omega)) d\mu \\ &= \mathbb{E}f(X) + \mathbb{E}Y\mathbb{E}f'(X) - \mathbb{E}(Xf'(X)) = \mathbb{E}(f(X) + (Y - X)f'(X)), \end{aligned} \quad (42)$$

which completes the proof. \square

Proof of Theorem 3.3. Let (Ω, μ) be a probabilistic space and $X: \Omega \rightarrow \mathbb{R}$ be a random variable. By the concavity of f we directly conclude that

$$f\left(\frac{1}{k+1} \sum_{i=1}^{k+1} x_i\right) = f\left(\frac{1}{k+1} \sum_{i=1}^{k+1} \frac{1}{k} \sum_{j=1, j \neq i}^{k+1} x_j\right) \geq \frac{1}{k+1} \sum_{i=1}^{k+1} f\left(\frac{1}{k} \sum_{j=1, j \neq i}^{k+1} x_j\right). \quad (43)$$

Then by monotonicity and linearity of the expected value, we obtain

$$\mathbb{E}f(\bar{X}_{k+1}) \geq \frac{1}{k+1} \sum_{i=1}^{k+1} \mathbb{E}f\left(\frac{1}{k} \sum_{j=1, j \neq i}^{k+1} X_j\right) = \mathbb{E}f(\bar{X}_k), \quad (44)$$

where X_1, \dots, X_{k+1} are independent copies of X . This gives the first assertion of the theorem.

Now consider the random variable \bar{X}_k . From the strong law of large numbers it follows that \bar{X}_k converges to $\mathbb{E}X$ almost surely. Hence, since f is continuous and the support of X is bounded, we conclude that $\mathbb{E}f(\bar{X}_k) \rightarrow f(\mathbb{E}X)$ as $k \rightarrow \infty$, which completes the proof. \square

Proof of Theorem 3.10. Let (Ω, μ) be a probabilistic space and $X, Y: \Omega \rightarrow \mathbb{R}$ be random variables satisfying the assumptions of the theorem. Put $m = \mathbb{E}X = \mathbb{E}Y$. By applying Taylor's expansion for f and f' , taking any $\omega \in \Omega$ we have

$$f(m) = f(X(\omega)) + (m - X(\omega))f'(X(\omega)) + \frac{1}{2}(m - X(\omega))^2 f''(X(\omega)) + o(\varepsilon^2) \quad (45)$$

and

$$f'(m) = f'(X(\omega)) + (m - X(\omega))f''(X(\omega)) + o(\varepsilon). \quad (46)$$

Hence,

$$f(m) = f(X(\omega)) + \frac{1}{2}(m - X(\omega))f'(m) + \frac{1}{2}(m - X(\omega))f'(X(\omega)) + o(\varepsilon^2). \quad (47)$$

Then integrating the above formula over all $\omega \in \Omega$ and making use the fact that X and Y are independent random variables with the same distribution, we obtain

$$f(\mathbb{E}X) = \mathbb{E}f(X) + \frac{1}{2}(\mathbb{E}X\mathbb{E}f'(X) - \mathbb{E}(Xf'(X))) + o(\varepsilon^2) = \mathbb{E}(f(X) + \frac{1}{2}(Y - X)f'(X)) + o(\varepsilon^2), \quad (48)$$

which completes the proof. \square

B Additional results

Experiments for VAE and IWAE models As we mentioned in Section 4 in the main paper, we compare the VAE model with the IWAE [6] models trained with two different numbers of samples: $k = 5$ (IWAE(5)) and $k = 10$ (IWAE(10)). For the IWAE models, we used the same neural architectures as in VAE. Table 3, which is an extension of Table 1 in the main paper, presents the full results (i.e. for various numbers of generated latent samples) of the mean and standard deviations of the lower and upper bounds of the log-likelihood for trained VAE, IWAE(5), and IWAE(10) models for all data sets considered.

Table 2: The means and standard deviations of lower and upper bounds of log-likelihood calculated from (6) (see the main paper) for trained VAE model for three datasets CelebA. In the columns named 'Lower' and 'Upper' we put the values of $\text{mean}(s_i) \pm \text{std}(s_i)$, $\text{mean}(S_i) \pm \text{std}(S_i)$ (calculated from (49)), respectively. As we can see, intervals shrink when we increase the number of samples. Moreover, the standard deviation is lower when we use large number of generated latent samples.

#samples	Lower	Upper	$\mathbb{E} \frac{X}{Y}$
1	-16158.75 ± 0.211	$8.05 \cdot 10^{17} \pm 5.263 \cdot 10^{17}$	$8.05 \cdot 10^{17} \pm 5.263 \cdot 10^{17}$
2	-16152.20 ± 0.317	$2.63 \cdot 10^{13} \pm 1.279 \cdot 10^{13}$	$2.63 \cdot 10^{13} \pm 1.279 \cdot 10^{13}$
4	-16147.31 ± 0.279	$4.86 \cdot 10^{10} \pm 2.034 \cdot 10^{10}$	$4.86 \cdot 10^{10} \pm 2.034 \cdot 10^{10}$
8	-16143.46 ± 0.231	$4.34 \cdot 10^8 \pm 2.336 \cdot 10^8$	$4.34 \cdot 10^8 \pm 2.336 \cdot 10^8$
16	-16140.36 ± 0.224	$1.82 \cdot 10^7 \pm 5.071 \cdot 10^6$	$1.82 \cdot 10^7 \pm 5.069 \cdot 10^6$
32	-16137.63 ± 0.184	$1.58 \cdot 10^6 \pm 4.288 \cdot 10^5$	$1.60 \cdot 10^6 \pm 4.288 \cdot 10^5$
64	-16135.24 ± 0.091	$2.46 \cdot 10^5 \pm 9.061 \cdot 10^4$	$2.62 \cdot 10^5 \pm 9.061 \cdot 10^4$
128	-16133.28 ± 0.141	53010.05 ± 9410.667	69143.57 ± 9410.337
256	-16131.56 ± 0.158	6055.59 ± 3486.470	22188.22 ± 3486.366
512	-16129.96 ± 0.313	-7051.54 ± 1438.311	9079.62 ± 1438.179
1024	-16129.21 ± 0.334	-11946.42 ± 774.333	4183.41 ± 774.302

Why is the improving upper bound for the variational gap needed? In Table 2 we show the mean and standard deviations of the upper and lower bounds estimates of the log-likelihood, calculated from (6) (see the main paper) for the VAE model trained on the CelebA dataset. Note that the values in the column named 'Upper' in Table 2 are larger than those in Table 3 for the VAE model. The reason for this is that the values in the column $\mathbb{E} \frac{X}{Y}$ in Table 2 are large. This justifies the need of reducing the width of the variational gap, which was done by introducing the estimate for the upper bound given in (27) (see the main paper).

Table 3: Means and standard deviations of lower and upper bounds for log-likelihood in trained VAE, IWAE(5) and IWAE(10) models, calculated for various numbers of generated latent samples, averaged over 10 times evaluations on random seed and 10,000 images from the test sets.

Dataset	Model	#samples	Lower	Upper	Gap
MNIST	VAE	32	-282.58 ± 0.109	-280.70 ± 0.742	1.93 ± 0.816
		64	-282.52 ± 0.063	-280.15 ± 0.887	2.44 ± 0.912
		128	-282.58 ± 0.083	-280.95 ± 0.660	1.64 ± 0.611
		256	-282.48 ± 0.079	-280.67 ± 0.667	1.90 ± 0.673
		512	-282.35 ± 0.119	-280.96 ± 0.599	1.49 ± 0.600
		1024	-282.27 ± 0.124	-280.88 ± 0.777	1.57 ± 0.792
	IWAE(5)	32	-284.34 ± 0.160	-283.67 ± 0.131	0.82 ± 0.090
		64	-284.27 ± 0.052	-283.49 ± 0.208	0.94 ± 0.202
		128	-284.26 ± 0.080	-283.54 ± 0.220	0.83 ± 0.157
		256	-284.13 ± 0.116	-283.61 ± 0.169	0.74 ± 0.122
		512	-284.08 ± 0.141	-283.66 ± 0.330	0.62 ± 0.296
		1024	-283.97 ± 0.082	-283.82 ± 0.086	0.35 ± 0.031
	IWAE(10)	32	-284.30 ± 0.145	-283.05 ± 0.295	1.29 ± 0.226
		64	-284.22 ± 0.132	-283.04 ± 0.198	1.21 ± 0.183
		128	-284.32 ± 0.129	-282.97 ± 0.374	1.36 ± 0.355
		256	-284.11 ± 0.171	-283.24 ± 0.619	0.99 ± 0.630
		512	-283.92 ± 0.168	-283.48 ± 0.184	0.63 ± 0.068
		1024	-283.88 ± 0.113	-283.63 ± 0.095	0.46 ± 0.052
SVHN	VAE	32	-4018.13 ± 0.311	-4011.67 ± 0.519	6.46 ± 0.642
		64	-4018.38 ± 1.189	-4011.18 ± 1.944	7.20 ± 1.046
		128	-4017.20 ± 0.941	-4009.24 ± 0.820	7.96 ± 0.808
		256	-4016.43 ± 0.839	-4010.20 ± 1.087	6.23 ± 0.467
		512	-4016.49 ± 0.505	-4010.97 ± 0.631	5.51 ± 0.334
		1024	-4015.35 ± 1.021	-4009.94 ± 1.325	5.41 ± 0.531
	IWAE(5)	32	-3994.04 ± 0.692	-3974.94 ± 0.794	19.10 ± 0.160
		64	-3994.40 ± 0.951	-3977.14 ± 3.302	17.25 ± 3.192
		128	-3992.62 ± 0.649	-3979.39 ± 2.695	13.23 ± 2.480
		256	-3992.40 ± 0.802	-3983.04 ± 0.883	9.36 ± 0.837
		512	-3991.61 ± 0.483	-3981.50 ± 2.563	10.11 ± 2.406
		1024	-3991.28 ± 0.571	-3982.01 ± 3.522	9.27 ± 4.068
	IWAE(10)	32	-3994.26 ± 0.154	-3979.66 ± 0.236	14.60 ± 0.082
		64	-3994.86 ± 0.656	-3978.42 ± 0.641	16.44 ± 0.182
		128	-3993.37 ± 0.813	-3978.46 ± 2.419	14.92 ± 2.756
		256	-3992.73 ± 0.378	-3977.65 ± 3.824	15.08 ± 3.703
		512	-3991.78 ± 0.678	-3981.87 ± 2.692	9.90 ± 2.804
		1024	-3990.94 ± 0.955	-3981.58 ± 2.722	9.36 ± 1.916
CelebA	VAE	128	-16154.91 ± 0.681	-15969.17 ± 118.905	182.65 ± 121.317
		256	-16146.98 ± 1.645	-15945.43 ± 163.788	199.06 ± 162.950
		512	-16143.63 ± 0.291	-16050.22 ± 60.270	91.02 ± 62.363
		1024	-16141.69 ± 5.193	-16115.50 ± 5.136	26.19 ± 1.683
	IWAE(5)	128	-16152.05 ± 1.512	-15693.38 ± 460.149	455.56 ± 460.642
		256	-16135.31 ± 0.116	-15911.07 ± 130.549	224.25 ± 147.864
		512	-16132.12 ± 0.113	-15994.97 ± 95.861	137.15 ± 98.957
		1024	-16140.56 ± 8.264	-16198.35 ± 8.581	57.79 ± 9.492
	IWAE(10)	128	-16143.52 ± 0.287	-15152.37 ± 270.713	989.42 ± 271.538
		256	-16152.70 ± 1.158	-15944.85 ± 171.329	203.69 ± 170.827
		512	-16146.88 ± 0.048	-15992.20 ± 98.486	151.48 ± 95.241
		1024	-16144.63 ± 7.394	-16206.11 ± 9.424	61.48 ± 8.745

C Experimental setup

Algorithmic details As we mentioned at the end of Section 4 in the main paper, to obtain the upper bound for the evidence, which can be updated additively, we use Theorem 3.8 for $X = \frac{1}{k} \sum_{i=1}^k R(x, z_i)$. Specifically, assuming that we have the sequence $(x_i)_{i=1, \dots, n}$ drawn from the data distribution, our algorithm can be described in the following steps. (We use here the notation established in Section 4.)

STEP 1. We construct a network which for x returns C_x for which the cost function given by $\sum_i GAP_{x_i}$ is minimized over x_i belonging to the training set.

STEP 2. Given a sequence $(x_i)_{i=1, \dots, n}$ drawn from the data distribution (in practice we take the testing set), our algorithm can be described as follows:

1. For each $i = 1, \dots, n$:
 - 1.1. for each $j = 1 \dots, k$, choose randomly z_{ij} and \tilde{z}_{ij} from the distribution $q(\cdot|x_i)$,
 - 1.2. compute:

$$s_i = \log \frac{1}{k} \sum_{j=1}^k R(x_i, z_{ij}), \quad S_i = s_i + C_{x_i} - 1 + \exp(-C_{x_i}) \frac{\sum_{j=1}^k R(x_i, \tilde{z}_{ij})}{\sum_{j=1}^k R(x_i, z_{ij})}. \quad (49)$$

2. Return the mean values \bar{s}_n and \bar{S}_n . Note that then

$$\mathbb{E}\bar{s}_n \leq \text{evidence of data} \leq \mathbb{E}\bar{S}_n. \quad (50)$$

Training details The experiments were performed on a single Tesla v100 GPU. We used a convolutional VAE architecture (for more details, see the next paragraph) with weights optimized by the Adam optimizer and a learning rate of 0.0001. The network is trained for 100 epochs with a batch size of 64 for CelebA dataset and 50 epochs for both MNIST and SVHN datasets. In all reported experiments, we used Euclidean latent spaces $\mathcal{Z} = \mathbb{R}^d$ for $d = 8, 32, 128$, depending on the used dataset (respectively: MNIST, SVHN and CelebA). We took standard Gaussian priors $p(z) \sim \mathcal{N}(\mathbf{0}, \mathbf{I}_d)$. We used Gaussian encoders $q(z|x) \sim \mathcal{N}(\mu_x, \Sigma_x)$, with a mean μ_x and a diagonal covariance matrix Σ_x , and Gaussian decoders $p(x|z) \sim \mathcal{N}(q(z|x), \sigma^2 \mathbf{I})$ with $\sigma^2 = 0.3$.

Architecture details for the experiments with VAE and IWAE models We used three different models, each for a different dataset. For the MNIST dataset, we use a network architecture that contains two parts: an encoder and a decoder. The encoder consists mainly of a 2-layer fully-connection, and the decoder consists of a 3-layer fully-connection. Between each layer, we use the ReLu activation function.

In the case of the SVHN dataset, we used a network deeper architectures encoder and decoder. Both networks consisted mainly of four-layer. The encoder had only convolution 2D, between which we used leaky ReLU with leakiness 0.2. In the decoder, we applied a 2D transposed convolution and ReLu as activation functions. For the last layer, we used the sigmoid activation function.

For the CelebA dataset, we used network architectures that consist mainly of replicated 5-layer blocks. In the encoder network, each block was built with a 2D convolution layer, batch normalization [14], and leaky ReLU with leakiness 0.2. A single block in the decoder network contained the upsampling operation that applies a 2D nearest-neighbour upsampling to an input signal composed of several input channels. Then, similar to the block of the encoder network, there was the 2D convolution layer, batch normalization, and leaky ReLU with leakiness 0.2. In all architectures, we described the parameters of the distribution (mean and standard deviation) in latent space as a single fully connected layer for each parameter.

Architecture details for the experiment with Laplace distributed variable To evaluate our method of bounding marginal likelihood, we have chosen $X \sim \text{Laplace}(0, 0.2)$ so that the likelihood can be easily calculated. We compare this likelihood estimated on 10^4 observations with ELBO, IWAE lower bound, and our proposed upper bound for $C = 0$ (without C correction) to judge how those bounds reflect the position of the real log-likelihood. To build lower and upper bounds, we sample different latent numbers of times to examine how a number of draws will affect bound positions. Moreover, for this problem, we selected batch of size 1000 and SGD optimizer with the learning rate 10^{-7} . The encoder consists of one hidden layer with 4 neurons and a ReLU activation function in it, with linear activation in the output layer. We set an identical network architecture for the decoder. The results are presented in Figure 2 in main paper that ELBO (green line) is placed at the bottom of the graph, below the lower and upper bounds (as expected). Another consistent with our logic phenomenon is that the IWAE lower bound and upper bound converge to the model log-likelihood, which is below the log-likelihood of true data (-0.097). The source of this discrepancy is driven by estimation error, which we have to always face when estimating any density (see the case study on synthetic data in the main paper). This experiment showed that the IWAE lower bound combined with our upper bound can efficiently bound the estimated log-likelihood, and these bounds are closer to its true value than the standard ELBO.